Int. J. Electrochem. Sci., 8 **(2013)** 3653 - 3663

International Journal of
ELECTROCHEMICAL
SCIENCE
www.electrochemsci.org

Prototype System for Magnesium/TiO_2 Anatase Batteries

E. Sheha

Physics Department, Faculty of Science, Benha University, Benha, Egypt
E-mail: e_sheha@yahoo.com

Received: 10 January 2013 / *Accepted:* 14 February 2013 / *Published:* 1 March 2013

In this work, a new polymer composite electrolyte films PCE are prepared based on poly(vinyl alcohol) (PVA), magnesium bromide $MgBr_2$, phosphomolbidic acid (PMA), and tetraethylene glycol dimethyl ether (TEGDME) using solution cast technique. The XRD are used to determine the complexation of the PVA polymer with Mg acid salt. The ionic conductivity of the composite films are determined by the complex impedance measurements in the temperature range 293–375 K. The ionic conductivity measurements revealed that the ionic conductivity of the electrolyte varies with the TEGDME concentration to reach the highest conductivity value of ~ 10^{-6} S. cm^{-1} at 303 K. The conductivity seems to follow the universal power law. The estimated value of Mg^+ ion transference number is carried out by the combination of complex impedance and D.C. polarization methods and is found to be 0.4 for high conducting film. A solid state battery based on the above polymer electrolyte with a configuration Mg|PCE|TiO_2 anatase has exhibited an open circuit voltage of 1.5 V. The discharge characteristics are found to be satisfactory as a laboratory cell.

Keywords: Polymer electrolyte; Magnesium ion conductor; Impedance spectroscopy; magnesium battery

1. INTRODUCTION

The supply of clean energy for our society is a central challenge to maintain our standing of living. It is important to change from fossil fuels to renewable energy sources for two main reasons: Firstly, the natural resources of gas and oil are limited and will run out. Secondly and more importantly, a continued dependence on fossil fuels would increase an already alarming rate of CO_2 emission. Additionally, other environmental problems such as oil spills, etc. caused by the mining of these resources may increase because the remaining resources will be in places which are more difficult to reach, e.g. far below sea level [1]. Rechargeable batteries are promising candidate for CO_2 emission free energy supply. However, the technology is still too expensive for their standing in competition against other energy sources [1].

Rechargeable Mg batteries have shown the potential for reversible electrochemical energy storage and conversion owing to their characters of high theoretical specific capacity (2205 $mAhg^{-1}$), great raw material abundance and good operational safety[2,3]. However, in comparison to Li-ion batteries, the major obstacles for rechargeable Mg batteries are the kinetically sluggish Mg intercalation/insertion and diffusion in cathode materials and the anode/electrolyte incompatibility duo to the high polarizing ability of the divalent Mg^{+2} cation [2,4]. In 2001, Prof. Aurbach et al. [4] reported attempts to construct rechargeable Mg battery systems based on $Mg(AlCl_3R)_2$ and $Mg(AlCl_2RR')_2$, where R and R' are alkyl groups—in tetrahydrofuran (THF) or polyethers of the glyme family solutions and a $Mg_xMo_3S_4$ intercalation cathode. However, much work need to exploit. Therefore, alternative material families, as well as new design approaches, are highly desirable for ultimate industrialization of Mg secondary batteries.

In this investigation, an attempt has been made to characterize the polymer electrolytes based on PVA complexed with magnesium bromide ($MgBr_2$), phosphomolbidic acid (PMA), and tetraethylene glycol dimethyl ether (TEGDME) at different weight percentages to evaluate their physio-chemical performance. In addition, solid-state Mg/PCE/TiO_2 anatase cell is assembled, and its cycling performances will be briefly examined to evaluate the applicability of the polymer electrolyte to solid-state magnesium batteries. X-ray diffraction mapping of the TiO_2 anatase electrode was measured before and after cycling.

2. EXPERIMENTAL SECTION

Poly (vinyl alcohol), PVA (degree of hydrolization ≥98%, Mw=72,000), magnesium bromide $MgBr_2$ and phosphmolbidic acid (PMA) were received from Sigma. The complex electrolytes were prepared by mixing of PVA, $MgBr_2$ and PMA at several stoichiometric ratios in distilled water to get $PVA_{(1-x)}(MgBr_2)_{x/2}(PMA)_{x/2}$ complex electrolytes, where *x* is 0.0, 0.1, 0.2, 0.3 gm. The solutions with variable ratio were stirred vigorously and casted in Petri dish following solution cast technique at room temperature. To the highest conducting composition in the polymer – acid salt system, different amount of TEGDME (x' = 0.0, 0.25, 0.5, 0.75 and 1 ml) were added to produce the plasticized electrolyte system.

The morphology of the polymer electrolyte was examined using scanning electron microscope, SEM (JOEL-JSM Model 5600).

The XRD patterns of the films were taken using SHIMADZU diffractometer type XRD 6000. The diffraction system based with Cu tube anode with voltage 40kV, current 30mA & wave length $K_{\alpha 1}$ = 1.5418 A°.

Conductivity measurements were made for $PVA_{(1-x)}(MgBr_2)_{x/2}(PMA)_{x/2}/_{x'}$TEGDME composite polymer membrane by impedance method. Samples of diameter 0.5 cm were sandwiched between the two similar stainless steel electrodes of a spring-loaded sample holder. The whole assembly was placed in a furnace monitored by a temperature controller. The rate of heating was adjusted to be 2 K min^{-1}. Impedance measurements were performed on PM 6304 programmable automatic RCL (Philips) meter in the frequency ranging from 100 Hz to 100 kHz at different temperatures.

Magnesium transference number (t_{Mg+2}) was measured by the steady-state technique which involved a combination of ac and dc measurements. The complex impedance response of the Mg/electrolyte/Mg cell was first measured to determine the cell resistances. It was followed by the dc polarization run, in which a small voltage pulse (ΔV=0.3V) was applied to the cell until the polarization current reached the steady-state. Finally, the complex impedance response of the cell was measured a gain to determine the cell resistance after dc polarization.

Electrodes with 70:30% TiO_2(aldrich anatase < 25 nm) /graphite and 20% electrolyte ($MgBr_2$ only) were prepared using the following protocol. A slurry obtained by mixing the TiO_2 /graphite / electrolyte solution is cast. The electrode is prepared by cold pressing 0.6 gm into a pellet of 13 mm in diameter under 2.5 tons/cm^2. The highest conducting electrolyte is deposited on the cathode substrate with a spin coater at 500 rpm. The anode was prepared by cold pressing 0.6 gm magnesium into a pellet of 13 mm in diameter under 2.5 tons/cm^2. Two-electrodes Swagelok test cell were assembled, the cell was discharged at room temperature on a multi-channel battery test system (NEWARE BTS-TC35) to analyze the electrochemical responses. The current density was 50 μA/cm^2.

3. RESULTS AND DISCUSSION

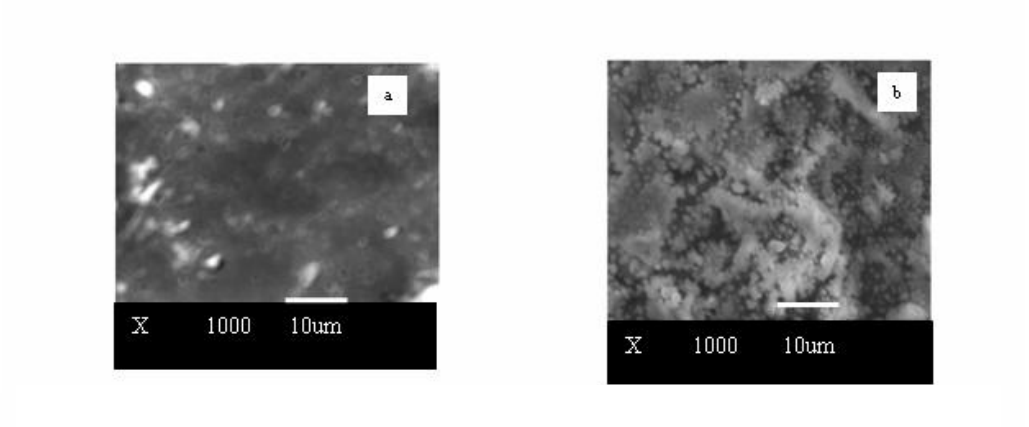

Figure 1. The SEM micrograph for the surface of $PVA_{0.7}(MgBr_2)_{x/2}(PMA)_{x/2}/_{x'}$ TEGDME acid salt membrane with (a) x=0.3, x'=0, (b) x=0.3, x'=1ml.

SEM was used to examine the morphology of two samples. Fig.1 shows the SEM images at a magnification factor 1000. The morphology of $PVA_{0.7}(MgBr_2)_{0.15}(PMA)_{0.15}$ displays a homogeneous surface with amorphous in nature. In contrast, the $PVA_{0.7}(MgBr_2)_{0.15}(PMA)_{0.15}/_{x'}$TEGDME membrane shows the formation of microstructures due to the interaction between the TEGDME and the polymer host.

Fig. 2 shows the XRD patterns of $PVA_{(1-x)}(MgBr_2)_{x/2}(PMA)_{x/2}$. The diffractogram of pure PVA (x=0) shows the presence of a semi-crystalline phase with the characteristic diffraction peak located at $2\theta=20^o$. Such semi-crystalline nature of PVA originates from the ordering of O-H group. On the other hand , in case of x > 0, the ordering in host PVA polymer is disrupted in presence of Mg acid salt due to coordination interaction between the acid salt and O-H group[5]. As a result a marked decrease in

the crystalliniy of $PVA_{(1-x)}(MgBr_2)_{x/2}(PMA)_{x/2}$ is observed compared to the pure PVA suggesting complete dissolving of the acid salt .

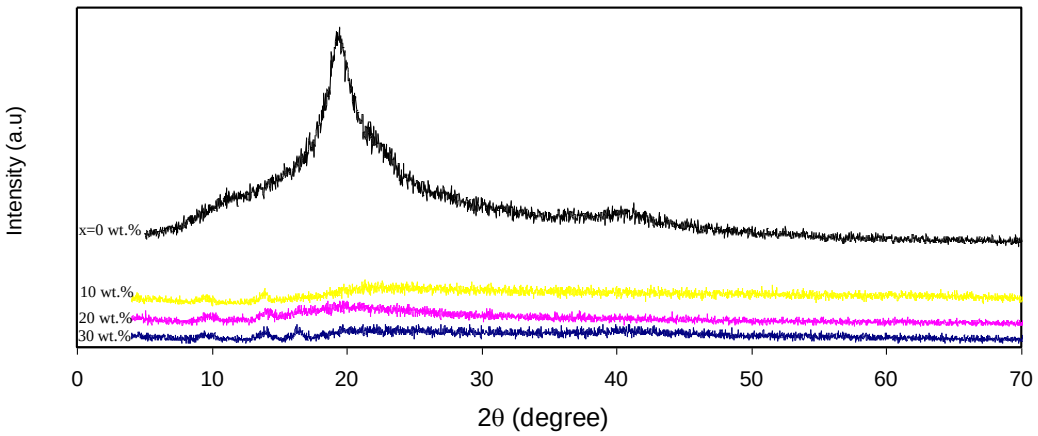

Figure 2. X-ray diffraction pattern for $PVA_{0.7}(MgBr_2)_{x/2}(PMA)_{x/2}$ membrane.

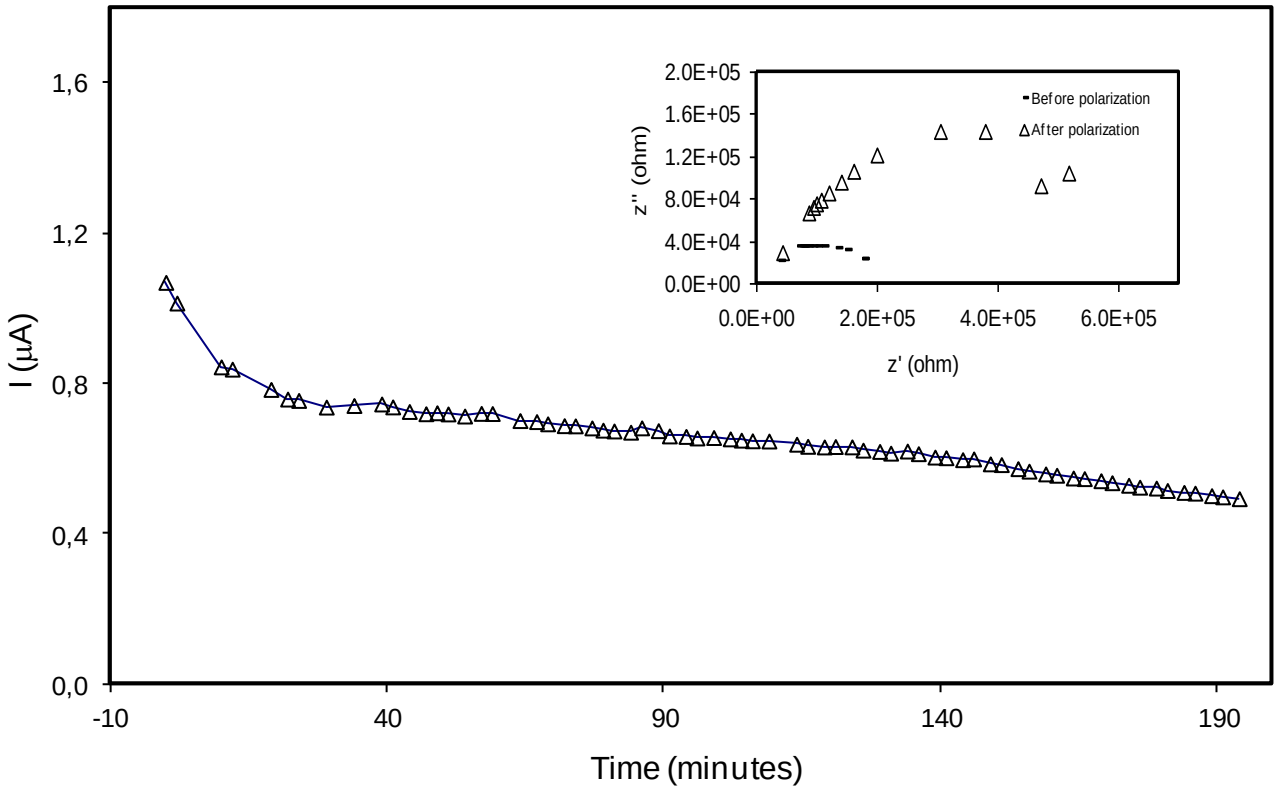

Figure 3. Variation of polarization current as a function of time for $PVA_{0.7}(MgBr_2)_{0.15}(PMA)_{0.15}/_{1ml}$TEGDME membrane.

The magnesium ion transference number (t_{mg}+) of the sample was measured at room temperature in the polymer electrolyte system, Fig. 3. Under real conditions current flow is also

affected by a passive layer forming, so the adequate correction for resistance changes is needed. Bruce and coworkers [6-8] introduced the following correction:

$$t_{mg^{2+}} = \frac{I_s(\Delta V - R_o I_o)}{I_o(\Delta V - R_s I_s)}$$

where ΔV is the D.C. voltage applied, R_0 is the passive layer resistance, R_s is the steady state passive layer resistance, I_0 is the initial current, and I_s is the steady state current. Impedance spectroscopy measurement was taken just before and after D.C. polarization and just after it reached steady state, Fig.3 (inset). In this study, the highest conducting electrolyte film showed t_{Mg+2} =0.4.

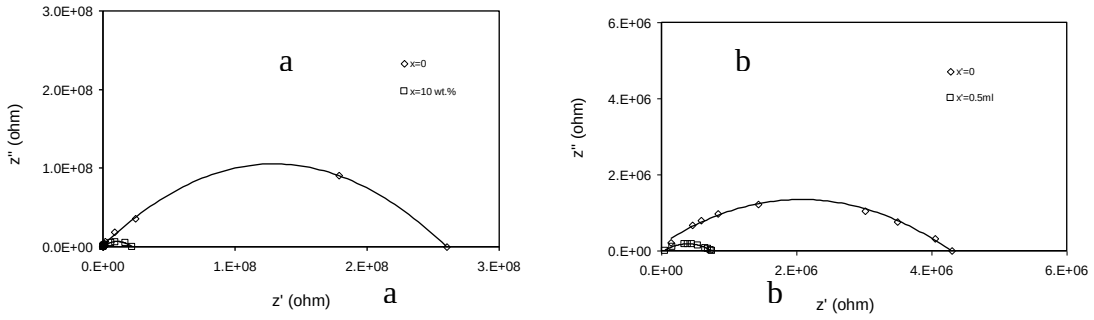

Figure 4. Cole Cole plots for $PVA_{(1-x)}(MgBr_2)_{x/2}(PMA)_{x/2}/_{x'}TEGDME$ films (a)x=0.0, 0.1, x'=0, (b)x=0.15, x'=0, 0.5

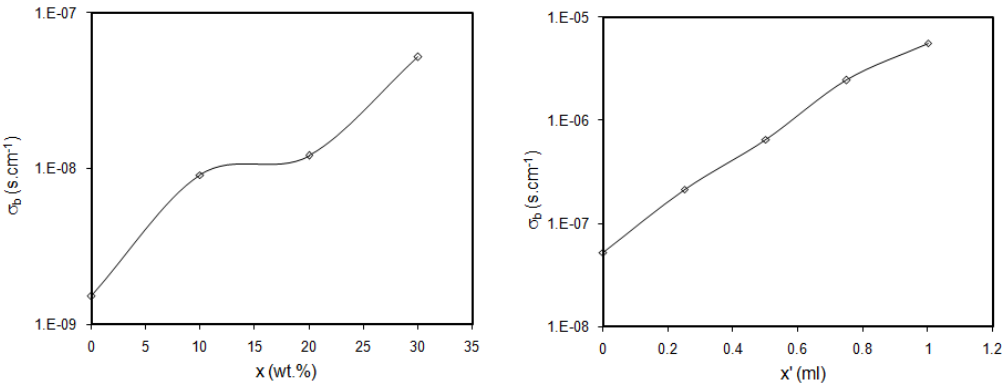

Figure 5. the ionic conductivity of $PVA_{(1-x)}(MgBr_2)_{x/2}(PMA)_{x/2}/_{x'}TEGDME$, (a) x'=0 and x ≠ 0, (b)x=0.5 and x'≠ 0.

Complex impedance plot of $PVA_{(1-x)}(MgBr_2)_{x/2}(PMA)_{x/2}/_{x'}TEGDME$ are shown in Fig.4 a and b. The complex plot shows semicircle which correspond to the bulk resistance R_b with parallel combination of the frequency dependent capacitance C_g. The bulk resistance value R_b is determined

from the low frequency intercepts on the x-axis of the complex impedance plots. The ionic conductivity is calculated using the equation $\sigma_b = \frac{1}{R_b} \times \frac{L}{A}$, where L is the thickness of the polymer electrolyte film, A is the surface area of the film.

Figs. 5 a,5b. show the bulk conductivity of $PVA_{(1-x)}(MgBr_2)_{x/2}(PMA)_{x/2}/_{x'}TEGDME$ electrolyte as a function of PMA and TEGDME content, respectively. The highest conductivity of $PVA_{(1-x)}(MgBr_2)_{x/2}(PMA)_{x/2}$ films is $\approx 10^{-7}$ $S.cm^{-1}$ and increased gradually with increasing the weight percentage of TEGDME. The highest conductivity of $PVA_{(1-x)}(MgBr_2)_{x/2}(PMA)_{x/2}/_{x'}TEGDME$ electrolyte film is $\approx 10^{-6}$ $S.cm^{-1}$ for the sample containing maximum loading of TEGDME amount. It is reasonable considering that the addition of TEGDME promotes Mg acid salt dissociation and weaken the Mg/Polymer bonds.

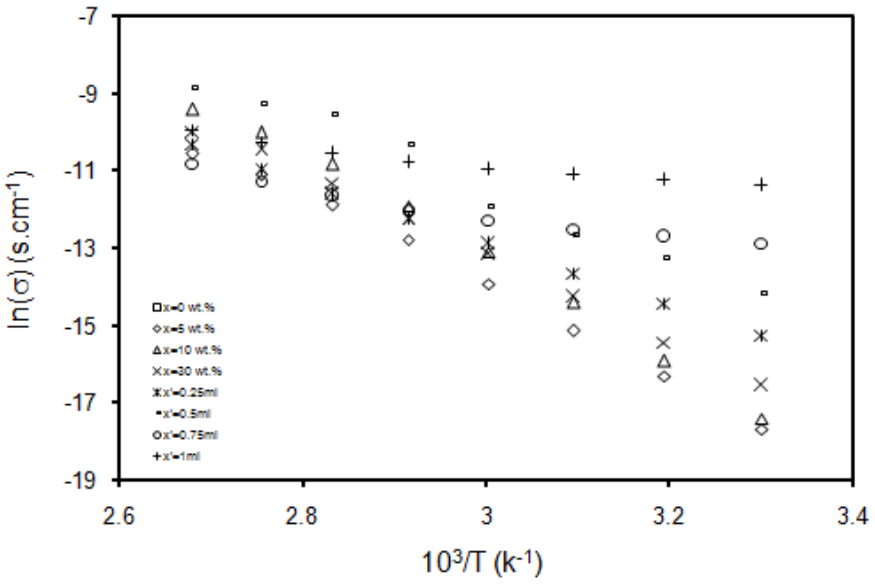

Figure 6. Arrhenius plot for $PVA_{0.7}(MgBr_2)_{x/2}(PMW)_{x/2}$ / $_{x'}TEGDME$ membrane.

Fig.6 shows the temperature - dependent ionic conductivity of $PVA_{(1-x)}(MgBr_2)_{x/2}(PMA)_{x/2}/_{x'}TEGDME$ electrolyte. From the plot, it is evident that, as temperature increase the conductivity also increases for all systems. The increase in conductivity with temperature has been explained in terms of segmental motion that result in increasing free volumes of the sample and the motion of ionic charge. The conductivity can be expressed as

$$\sigma_b = \sigma_0 \exp\left(\frac{-E_a}{k_B T}\right)$$

where σ_o denotes the pre-exponential factor, E_a is the energy of activation for conduction, K_B is Boltzmann constant and T is the temperature in Kelvin. As shown in Fig.6 the data are fitted well into one region for $PVA_{(1-x)}(MgBr_2)_{x/2}(PMA)_{x/2}$ and into two regions for

$PVA_{0.7}(MgBr_2)_{0.15}(PMA)_{0.15}/_{x'}$TEGDME. This may be attributed to the difference in the melting point before and after doping by TEGDME. Activation energy at different concentrations of Mg acid salt and TEGDME was obtained using Arrheius relationship.

Table 1. Activation energy, conduction index and dc conductivity for $PVA_{(1-x)}(MgBr_2)_{x/2}(PMA)_{x/2}/_{x'}$TEGDME membrane.

x wt.%	E_1	E_2	n_1	n_2	σ_{dc}
0	0.84	-	0.0481	1.7346	$1.3x10^{-9}$
10	1	-	0.375	1.0525	$4.1x10^{-10}$
20	1.1	-	0.1968	0.7988	$2.3x10^{-9}$
30	0.94	-	0.0706	0.5838	$3.4x10^{-8}$
x=30 wt.%, x'~variable					
0.25ml	0.675716	0.707022	0.0371	0.4053	$1.3x10^{-7}$
0.5ml	0.633471	0.498976	0.0435	0.3101	$5x10^{-7}$
0.75ml	0.151921	0.382679	0.0147	0.1588	$2.4x10^{-6}$
1ml	0.12399	0.271456	0.0121	0.0659	$1x10^{-5}$

Table 1 presents a comparison of the activation energy data, it can be observed that the lowest activation energy is for the film doped with 1 ml TEGDME, which indicate that TEGDME have effect on Mg^+X^- dissociation and ionic transfer.

Fig.7 shows the frequency - dependent conductivity of $PVA_{(1-x)}(MgBr_2)_{x/2}(PMA)_{x/2}/_{x'}$TEGDME polymer electrolyte. It seems to follow a universal power law[9]

$$\sigma_{ac} = \sigma_o + A\omega^n$$

where σ_o is the dc conductivity(the extrapolation of the plateau region to zero frequency gives the value of dc ionic conductivity), A is the pre-exponential factor and n the fractional exponent lying between 0&1. The calculated values of n and σ_o (using fitting technique) as a function of Mg acid salt and TEGDME concentration are listed in Table1. It is clear that σ_o increases with increase Mg acid salt and TEGDME concentration, while, n decreases with increase them. The calculated values of

power law exponent n, generally for ionic conductor can be between 1.0 and 0.5, indicating the ideal long-range path way diffusion limited hopping.

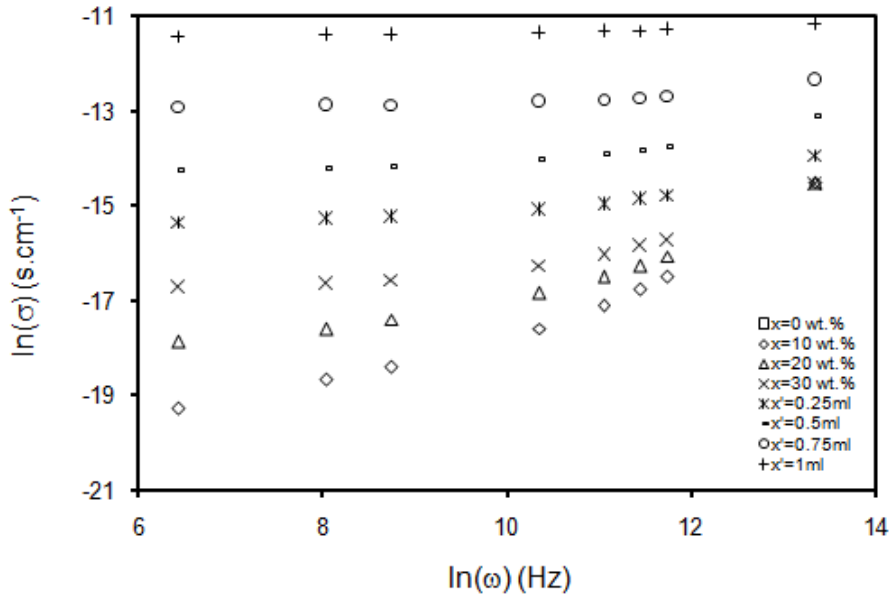

Figure 7. Variation of conductivity with frequency for $PVA_{0.7}(MgBr_2)_{x/2}(PMW)_{x/2}$ / $_{x'}$TEGDME membrane.

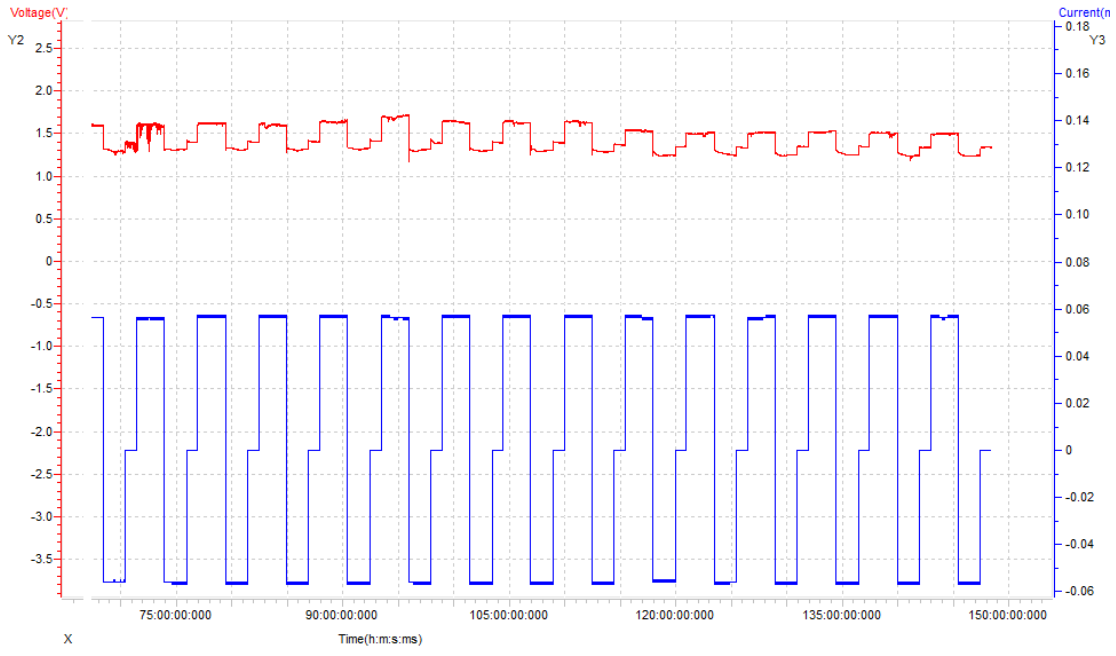

Figure 8. Charge - discharge curves of a Mg / PCE / TiO_2 anatase cell at room temperature.

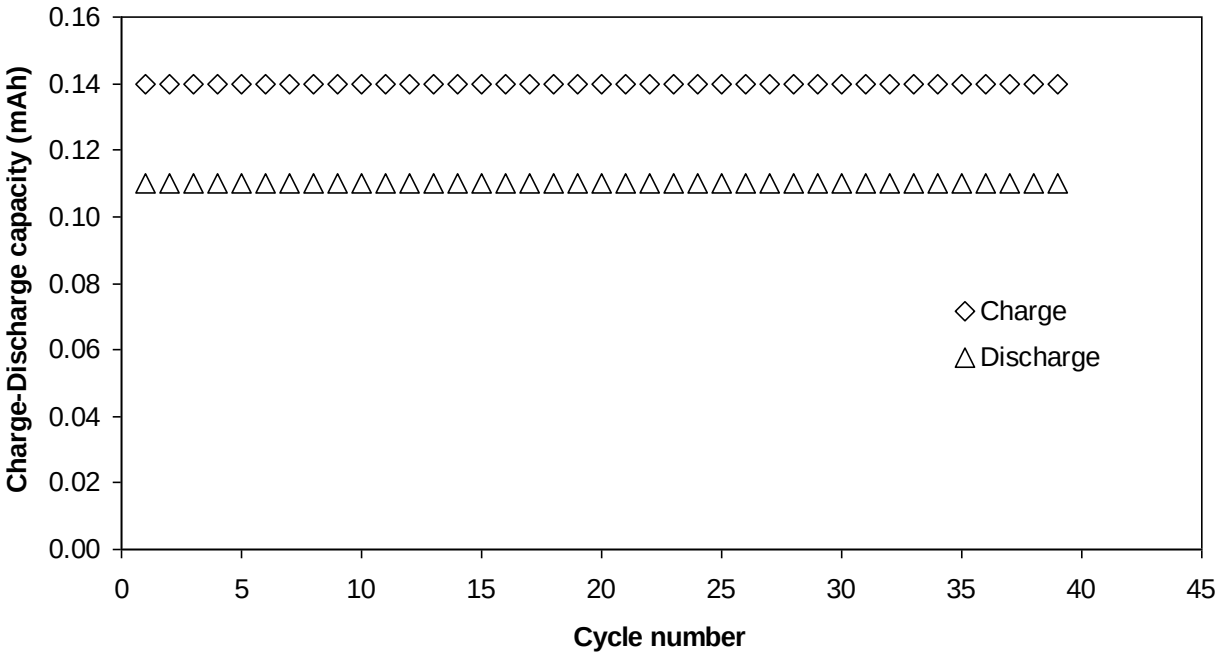

Figure 9. Typical cycling behaviour of the cell fabricated.

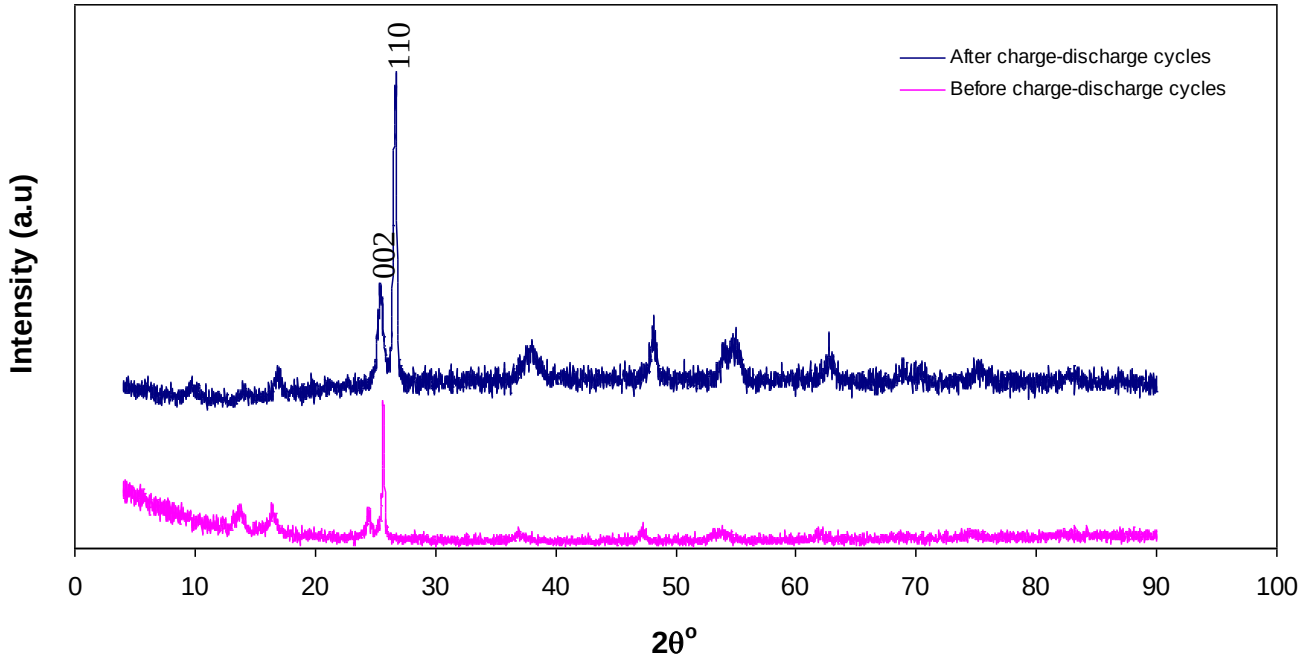

Figure 10. X-ray diffraction pattern for TiO2 cathode before and after cycling.

If n=0 the motion completely random and independent Debye like ion hops. In the present case n was found > 0.5 for $PVA_{(1-x)}(MgBr_2)_{x/2}(PMA)_{x/2}$ and n $\rightarrow$0 due to doping by TEGDME. Therefore, there are two mechanisms of conduction. The first is jump relaxation model. According to jump relaxation model, at very low frequencies ($\omega \rightarrow 0$) an ion can jump from one site to its neighboring site successfully contributing to the dc conductivity[10]. At higher frequencies, the probability for the ion

go back again to its initial site increases due to the short time periods. The high probability for the correlated forward-backward hopping at higher frequencies together with the relaxation of the dynamic cage potential is responsible for the observed high frequency conductivity-dispersion. On the other hand, in the presence of TEGDME the mechanism of conduction make transition from jump relaxation model to liquid model, where the motion is frequency independent.

In order to examine the applicability of the composite polymer electrolyte to rechargable magnesium battery system , we fabricated prototype cell consisting of TiO_2 anatase (< 25 nm) cathode, Mg metal anode and the highest conducting electrolyte film. The electrochemical insertion of divalent Mg^{2+} cations into TiO_2 anatase has not been reported in the literature. The open circuit voltage of the the Mg/TiO_2 anatase has been observed to be around 1.5 V. Fig. 8 shows typical discharge and recharge curves of the Mg/TiO_2 anatase cell under constant current condition. The cycle life data of Mg/TiO_2 anatase is shown in Fig. 9. The data show stable charge-discharge cycles.

Fig. 10 shows the x-ray powder diffraction (XRD) pattern of TiO_2 anatase cathode before and after cycling. It can be seen that there are significant difference between them. There is a noticable shift of 002 (graphite)[11] and 110 (TiO_2 anatase) [11] planes towards higher diffraction angle for the cathode after cycling corresponding to decrease of the interlayer distance from 3.470 Å to 3.34 Å, table 2.

Table 2. Lattice constans and particle sizes of TiO_2 anatase cathode befor and after cycling.

no.	Lattice constant d (Å)		Particle size (nm)	
	Pure	Discharge	Pure	Discharge
1	3.47065	3.34576	42.39627	24.05074
2	3.64363	3.50563	31.24937	15.26371
3	5.36822	1.89015	22.28954	22.4938

We calculated the crystallite sizes D for TiO_2 electrode before and after cycling using Scherrer equation[12]:

$$D = 0.9\,\lambda/(B.\cos\theta)$$

where 0.9 is the Scherrer constant, λ is the wavelength of X-ray, B is the breadth of the pure diffraction profile and θ is the incidence angle of the X-ray. The results are listed in Table 2. This reduction in the crystallite size can be attributed to the strain experience due to the intercalation of Mg^{+2} with TiO_2 anatase.

4. CONCLUSION

We successfully demonstrated the approach of combining a polymer and a plastic crystal to generate a new type of magnesium ion conductor. The addition of TEGDME can obviously increase

the ionic conductivity of the polymer. The ionic conductivity depended on the content of TEGDME. The highest conductivity of the PCE examined was $\approx 10^{-6}$ S. cm^{-1} (at 303 K). The present results are only the first step in the exploration of these materials. Further work is in progress to increase the specific capacity and cyclapility by modifications.

ACKNOWLEDGMENT
We are grateful to the Science technology development fund of Egypt, grant number 2069.

References

1. B. Scrosati, *Nature*, 2(2007)598.
2. W. Li, C. Li, C. Zhou, H. Ma, J. Chen, *Angew Chem*, 45 (2006)6009.
3. Y. Liang, R. Feng, S. Yang, H. Ma, J. Liang, *J. Chen, Adv Mater*, 23 (2011)640.
4. D. Aurbach, Z. Lu, A. Schechter, Y. Gofer, H. Gizbar, R. Turgeman and et al, *Nature*, 407 (2000)724.
5. E. Sheha, *J Non-Cryst Solids*, 356 (2010)2282.
6. M. Varishetty, W. Qiu, Y. Gao, W. Chen, *Polym Eng Sci* (2010)879.
7. P. Bruce, C. Evans, *Electroanal. Chem. Interf. Electrochem*, 225(1987)1.
8. S. Panero, B. Scrosati, H. Sumathipala, W. Wieczorek, *J. Power Sources*, 167(2007)510.
9. A. K. Jonscher, The 'universal' dielectric response, *Nature*, 267(1977)673.
10. K. Pandey, M. Dwivedi, M. Singh, S. Agrawal, *J Polym Res*, 17 (2010)127.
11. C. Tao, L. Fan, X. Yan, X. Qu, *Electrochim Acta*, 69(2012)328.
12. S. Kitazawa, Y. Choi, S. Yamamoto, T. Yamaki, *Thin Solid Films*, 515(2006)1901.